NOAA Technical Report NOS 87 NGS 18

Crustal Movement Investigations at Tejon Ranch, California

Rockville, Md.
June 1980

U.S. DEPARTMENT OF COMMERCE
National Oceanic and Atmospheric Administration
National Ocean Survey

NOAA Technical Publications

National Ocean Survey/National Geodetic Survey subseries

The National Geodetic Survey (NGS) of the National Ocean Survey (NOS), NOAA, establishes and maintains the basic National horizontal and vertical networks of geodetic control and provides governmentwide leadership in the improvement of geodetic surveying methods and instrumentation, coordinates operations to assure network development, and provides specifications and criteria for survey operations by Federal, State, and other agencies.

NGS engages in research and development for the improvement of knowledge of the figure of the Earth and its gravity field, and has the responsibility to procure geodetic data from all sources, process these data, and make them generally available to users through a central data base.

NOAA Technical Memorandums and some special NOAA publications are sold by the National Technical Information Service (NTIS) in paper copy and microfiche. Orders should be directed to NTIS, 5285 Port Royal Road, Springfield, VA 22161 (telephone: 703-557-4650). NTIS customer charge accounts are invited; some commercial charge accounts are accepted. When ordering, give the NTIS accession number (which begins with PB) shown in parentheses in the following citations.

Paper copies of NOAA Technical Reports, that are of general interest to the public, are sold by the Superintendent of Documents, U.S. Government Printing Office (GPO), Washington, DC 20402 (telephone: 202-783-3238). For prompt service, please furnish the GPO stock number with your order. If a citation does not carry this number, then the publication is not sold by GPO. All NOAA Technical Reports may be purchased from NTIS in hard copy and microform. Prices for the same publication may vary between the two Government sales agents. Although both are nonprofit, GPO relies on some Federal support whereas NTIS is self-sustained.

An excellent reference source for Government publications is the National Depository Library program, a network of about 1,300 designated libraries. Requests for borrowing Depository Library material may be made through your local library. A free listing of libraries currently in this system is available from the Library Division, U.S. Government Printing Office, 5236 Eisenhower Ave., Alexandria, VA 22304 (telephone: 703-557-9013).

NOAA geodetic publications

Classification, Standards of Accuracy, and General Specifications of Geodetic Control Surveys. Federal Geodetic Control Committee, John O. Phillips (Chairman), Department of Commerce, NOAA, NOS, 1974 reprinted annually, 12 pp (PB265442). National specifications and tables show the closures required and tolerances permitted for first-, second-, and third-order geodetic control surveys. (A single free copy can be obtained, upon request, from the National Geodetic Survey, OA/C18x2, NOS/NOAA, Rockville, MD 20852.)

Specifications To Support Classification, Standards of Accuracy, and General Specifications of Geodetic Control Surveys. Federal Geodetic Control Committee, John O. Phillips (Chairman), Department of Commerce, NOAA, NOS, 1975, reprinted annually, 30 pp (PB261037). This publication provides the rationale behind the original publication, "Classification, Standards of Accuracy, ..." cited above. (A single free copy can be obtained, upon request, from the National Geodetic Survey, OA/C18x2, NOS/NOAA, Rockville, MD 20852.)

Proceedings of the Second International Symposium on Problems Related to the Redefinition of North American Geodetic Networks. Sponsored by U.S. Department of Commerce; Department of Energy, Mines and Resources (Canada); and Danish Geodetic Institute; Arlington, Va., 1978, 658 pp. (GPO #003-017-0426-1). Fifty-four papers present the progress of the new adjustment of the North American Datum at midpoint, including reports by participating nations, software descriptions, and theoretical considerations.

NOAA Technical Memorandums, NOS/NGS subseries

NOS NGS-1 Use of climatological and meteorological data in the planning and execution of National Geodetic Survey field operations. Robert J. Leffler, December 1975, 30 pp (PB249677). Availability, pertinence, uses, and procedures for using climatological and meteorological data are discussed as applicable to NGS field operations.

NOS NGS-2 Final report on responses to geodetic data questionnaire. John F. Spencer, Jr., March 1976, 39 pp (PB254641). Responses (20%) to a geodetic data questionnaire, mailed to 36,000 U.S. land surveyors, are analyzed for projecting future geodetic data needs.

(Continued at end of publication)

NOAA Technical Report NOS 87 NGS 18

Crustal Movement Investigations at Tejon Ranch, California

Richard A. Snay
Michael W. Cline

Rockville, Md.
June 1980

U. S. DEPARTMENT OF COMMERCE
Philip M. Klutznick, Secretary

National Oceanic and Atmospheric Administration
Richard A. Frank, Administrator

National Ocean Survey
Herbert R. Lippold, Jr., Director

PREFACE

The text of this report was released in an earlier, unpublished form under the title "California Aqueduct-Fault Crossing Study, Section IV: Sandburg to Wheeler Ridge, Supplement No. 9, Ranch-Tejon Site." The title was changed largely because the original report (Parkin 1966) and its eight later supplements (Miller 1966-1976), all unpublished, are based on individual epochs of data. The title change also helps to emphasize the new adjustment approach, presented herein, that allows all the epochs of data to be combined into a unified whole.

ERRATA

September 11, 1980

p. 8, change last paragraph to read

Here t_o is a fixed time of reference, and $(\phi_{t_o}, \lambda_{t_o})$ are the geodetic coordinates of the station at time t_o. Each $f_{i,j}$ for $1 \leq j \leq 4$ is a function of the variables ϕ_{t_o} and λ_{t_o} and is of the form

p. 16, change paragraph 5 to read

The next set of adjustments seeks to model accurately the 1969-78 motion of the RANCH-TEJON-2 network.

p. 20, line 25, change last equation to read

$$F_{2,770} = \frac{(1432.8-1401.0)/(772-770)}{1401.0/770} = 8.74$$

p. 20, line 26, change the number 8.635 to 8.74

CONTENTS

FIGURES

TABLES

CRUSTAL MOVEMENT INVESTIGATIONS AT TEJON RANCH, CALIFORNIA

Richard A. Snay
Michael W. Cline

National Geodetic Survey
National Ocean Survey, NOAA
Rockville, Md. 20852

ABSTRACT. From 1964 to 1978, the National Geodetic Survey has observed during 10 epochs two small and recently interconnected networks, RANCH and TEJON, which span two branches of the Garlock fault in California's Tehachapi Mountains. The 10 epochs of data, simultaneously adjusted using the least-squares methods and with the faults mathematically modeled, show that the horizontal crustal motion has varied nonlinearly with respect to time. The southern branch of the Garlock fault, spanned by the RANCH network, exhibited left-lateral strike slip and dip slip corresponding to normal faulting. Subsidence measured by vertical observations at this branch indicates that the fault dips southerly.

INTRODUCTION

Under a cooperative agreement between the National Oceanic and Atmospheric Administration (NOAA) and the State of California Department of Water Resources, the National Geodetic Survey (NGS) has established 30 fault-crossing networks in various areas of the San Andreas fault system. Each of these periodically reobserved networks consists of six to eight geodetic stations with sides of the figures ranging in length from 200 to 900 meters. Two of these fault-crossing networks, the recently interconnected Site 13, RANCH, and Site 14, TEJON, are the subject of this ninth supplement to the June 1966 unpublished report "Results of Triangulation for Earth Movement Study at California Aqueduct-Fault Crossing Sites - Section IV: Sandburg to Wheeler Ridge" (Parkin 1966).

The two sites are located, appropriately enough, on the Tejon Ranch, near latitude 34° 53' and longitude 118° 47', in the rugged foothills of the Tehachapi Mountains. The RANCH and TEJON sites lie about 7 miles northeast of Lebec, where each net is located at opposite ends of an aqueduct water tunnel. The TEJON site is positioned at the northern aqueduct entrance, and RANCH is to the south. Together they straddle two branches of the Garlock fault.

Originally, the TEJON site consisted of seven stations, TEJON-A continuing alphabetically through TEJON-G, which were observed annually from 1964 to 1966. But during 1967, aqueduct construction destroyed all but TEJON-B. Then in 1970, a new TEJON site assimilating the original TEJON-B was established in the same vicinity but was enlarged to cover a greater area. In this supplement, the original TEJON site will be referred to as TEJON-1, and the new network will be called TEJON-2.

Separate surveys at the other site, RANCH, were made annually from 1964 to 1969. Then in 1972, 1975, and 1978, the two networks, RANCH and TEJON-2, were combined into a single network, which also contains six stations positioned by other networks. It is this network, RANCH-TEJON-2, that straddles both branches of the Garlock fault.

FIELD WORK

The general locations and configurations of the original RANCH and TEJON sites are shown in figures 1 and 2 of the June 1966 report. Figure 1A of this report is a portion of a geological map of California--Los Angeles Sheet 1971, State of California Department of Conservation. Figure 1B is an enlargement of the outlined area in figure 1A showing the RANCH-TEJON site; figure 2 shows a large-scale sketch of the RANCH-TEJON-2 network.

The dates of the 1978 survey were from May 18 to July 19, 1978. The survey specifications are quoted as follows:

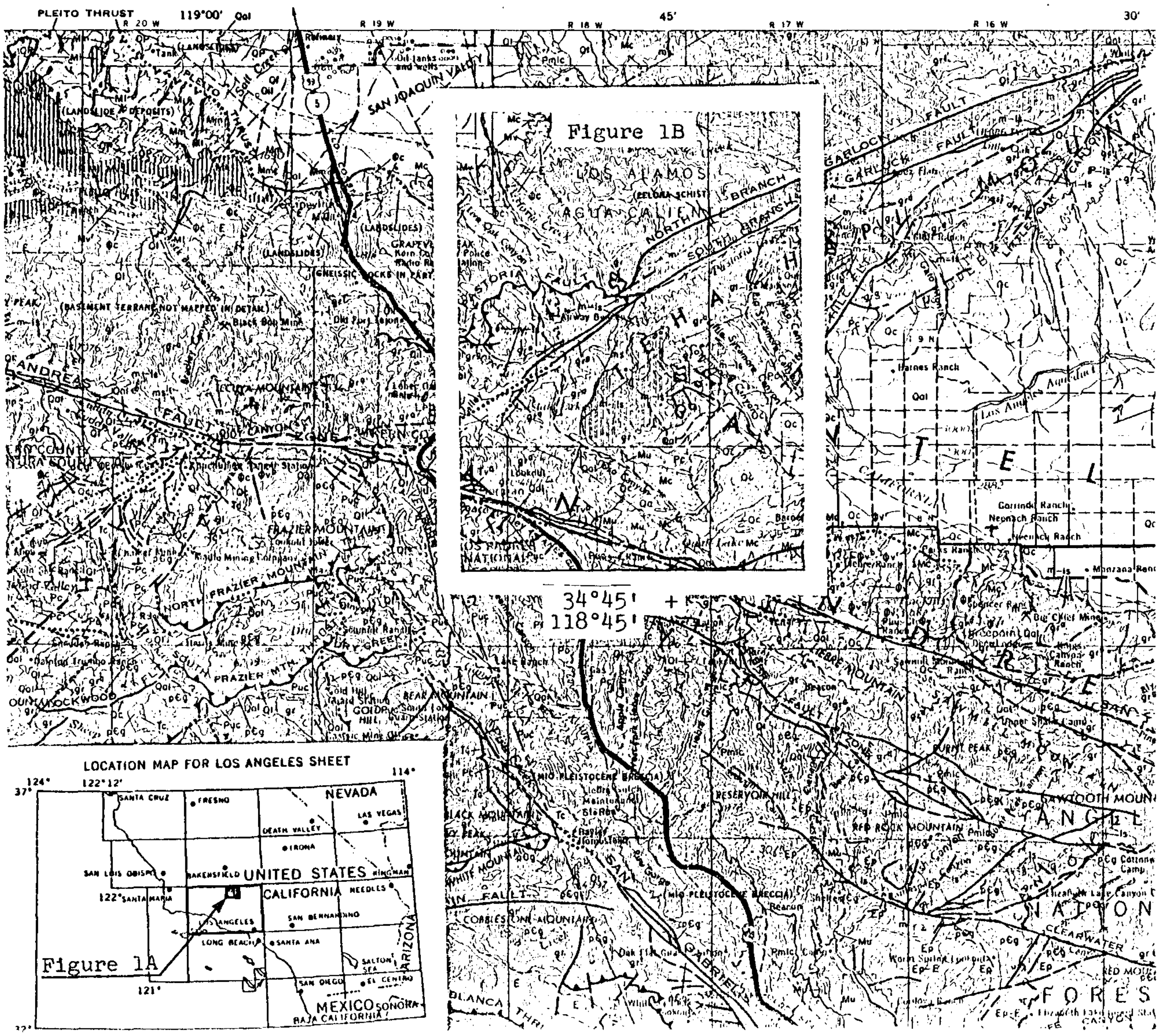

Figure 1A.--General location of RANCH-TEJON site.

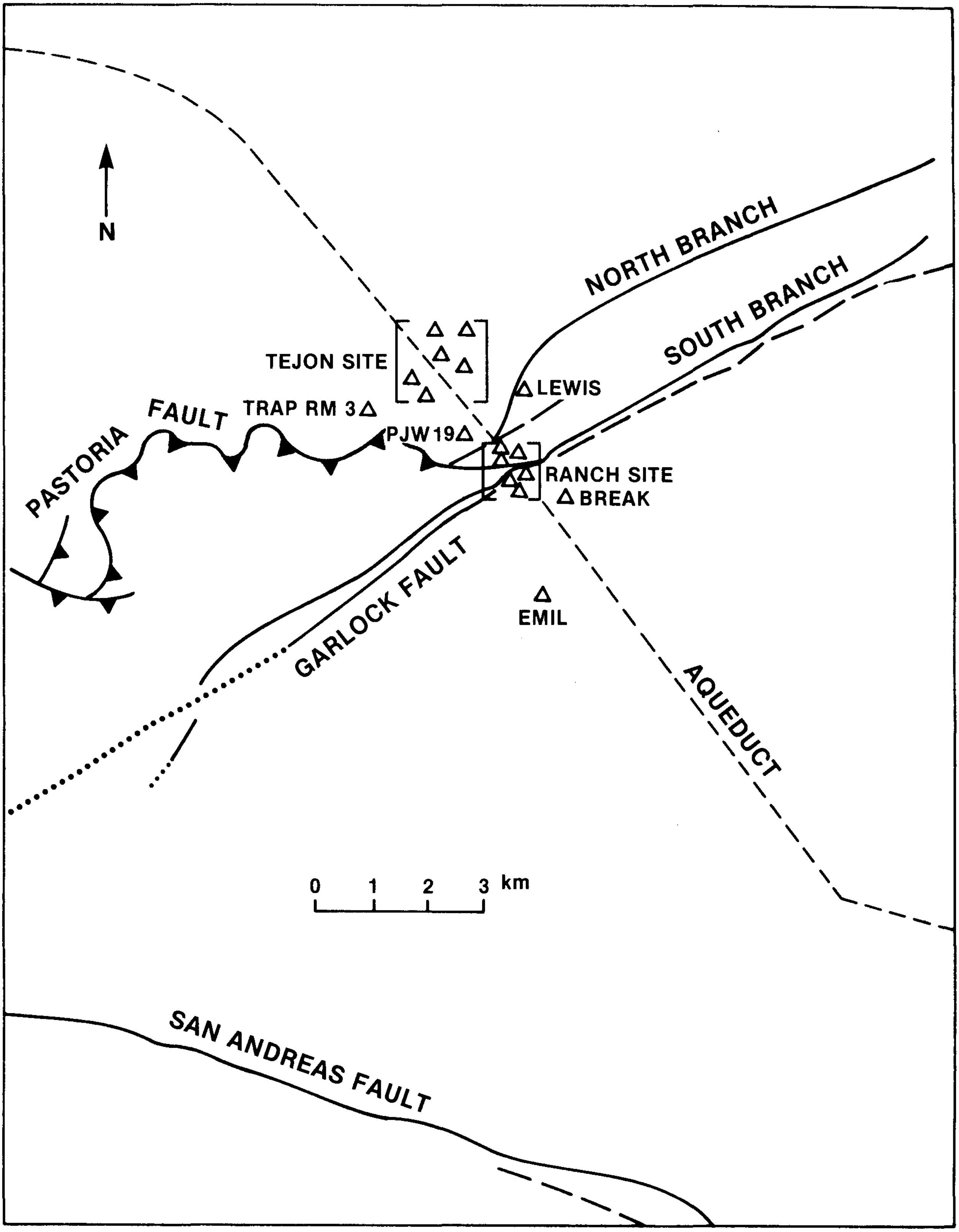

Figure 1B.--Location and plan of RANCH-TEJON-2 site.

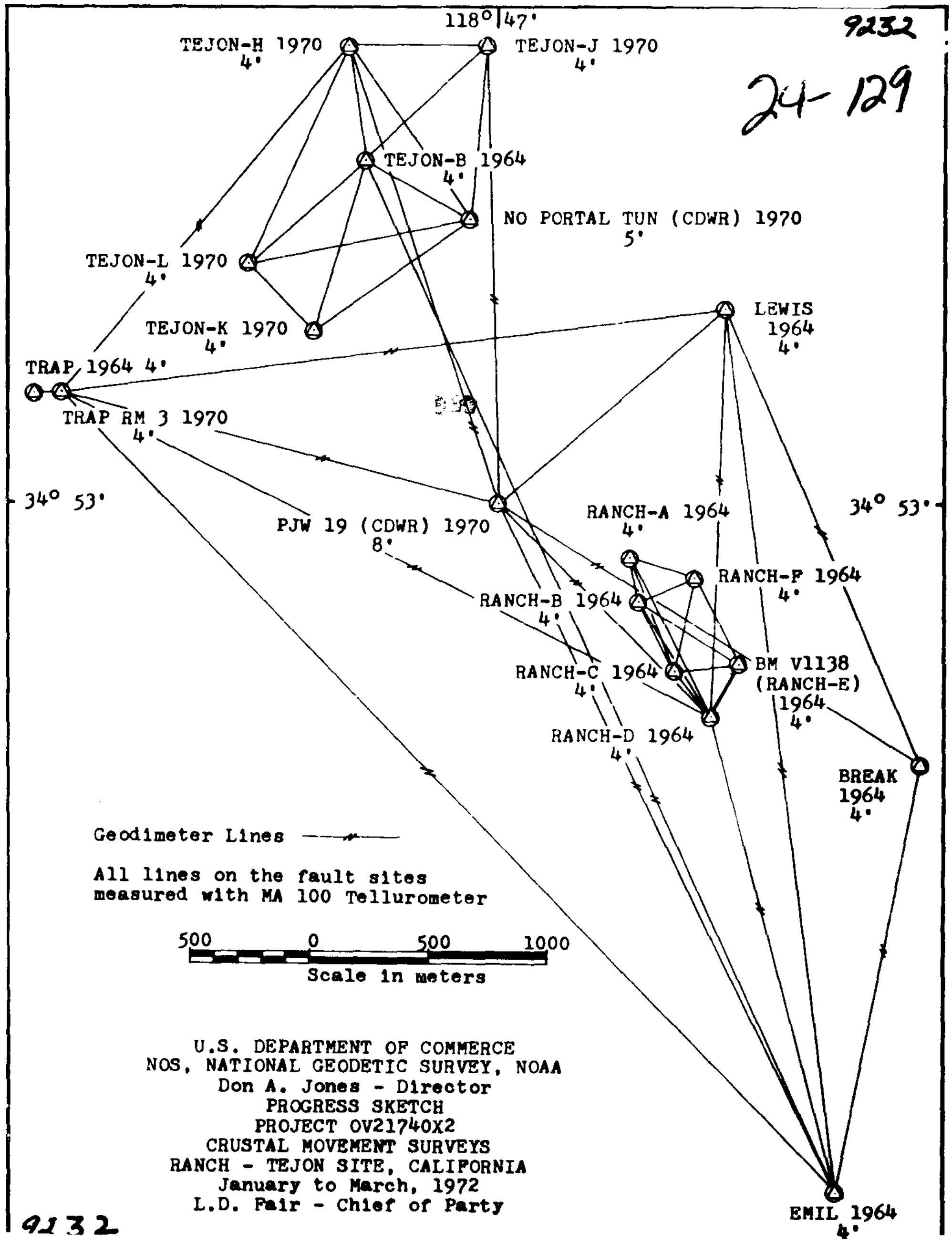

Figure 2.--Triangulation-trilateration plan of RANCH-TEJON-2 site.

The site will be observed by both triangulation and trilateration methods. Direction observations will be made over all lines on a single occasion using first-order procedures. Each line (distances) will be measured in both directions employing a different instrument at each end. The short lines will be observed with MA100 Tellurometers and the longer lines using Geodimeters. The spread between the mean of the complete observations at each end of the line will rarely exceed 5 mm + 1 ppm of the distance for MA100 measurements and 10 mm + 1 ppm where Geodimeters are employed. Measurements will be made where it is practical to do so during the period 1/2 hour to 2 hours before sunset. Where the distances are measured in one direction during the day (more than 2 hours prior to sunset) and in the other direction during the night (dusk or later), the spreads should not exceed 10 mm + 1 ppm of the distance for MA100 observations and 15 mm + 1 ppm for those lines measured using Geodimeters. Where possible, the distance measurements over the same lines should be obtained on different days/ nights. Direction observations may be made during the day if refraction conditions permit. The triangulation and trilateration will conform to first-order standards.

Observations will be secured as detailed in Classification, Standards of Accuracy and General Specifications of Geodetic Control Surveys (Federal Geodetic Control Committee 1974) and Specifications to Support Classification, Standards of Accuracy and General Specifications of Geodetic Control Surveys (Federal Geodetic Control Committee 1975), except as modified above and as follows. Triangle closures in the small figures (TEJON-RANCH sites) shall not exceed 5", and the average shall not exceed 2". Evaluation of the triangulation and trilateration will be made following the procedures outlined in "Tests on Trilateration Surveys to be Made in the Field." The lines LEWIS 1964 - PJW 19 (CDWR) 1970 and LEWIS 1964 - RANCH-D 1964 will be measured with both the MA100 Tellurometers and the Geodimeters as a check on the instruments. No taped distances are required over any of the regular lines of the net. Leveling will consist of re-observing the original surveys in accordance with leveling instructions titled "Special Instructions for Leveling at Hollister - Type Figures."

The surveys required at the TEJON-RANCH site (combined in 1970) consist of the following:

1. Observe an astronomic azimuth at TEJON-B, using TEJON H, K, and J as ground stations.

2. Observe an astronomic azimuth at RANCH-E, using RANCH-D, C, B, and F as ground stations.

3. All lines within the RANCH site will be measured with at least two MA100 instruments.

4. All lines within the TEJON site will be measured with at least two MA100 instruments.

5. Lines connecting the TEJON site to the RANCH site will be measured with each of two Geodimeters.

6. Each station mark at the sites will be carefully examined visually to determine if any local disturbance has occurred, and each recovery note should contain a statement to this effect.

In 1978, all stations were reported in good condition with no noticeable crustal movement found in the vicinity of any of the stations.

For the survey specifications and other details of previously reported surveys, see the individual supplements (Miller 1966-68, 1970, 1972, 1976).

Table 1 gives a summary of all the horizontal field work data taken at the RANCH-TEJON site. Table 2 summarizes the vertical field work data.

Table 1.--Horizontal field work

Site	Date of survey	Stations	Directions	Distances	Azimuths
RANCH	May 1964	6	50	1	1
TEJON-1	May 1964	7	54	1	1
RANCH	March 1965	6	43	1	1
TEJON-1	March 1965	7	43	1	1
RANCH	April-May 1966	6	71	3	1
TEJON-1	April-May 1966	7	91	3	1
RANCH	June 1967	6	64	8	1
RANCH	June 1968	6	56	5	1
RANCH	April-May 1969	6	61	5	1
TEJON-2	June-July 1970	13	122	29	1
RANCH-TEJON-2	January-March 1972	18	243	69	2
RANCH-TEJON-2	March-April 1975	18	38	94	2
RANCH-TEJON-2	May-July 1978	18	184	187	5

Table 2.--Vertical field work

Site	Date of survey
RANCH-TEJON-2	June-August 1971
RANCH-TEJON-2	January-February 1972
RANCH-TEJON-2	March-April 1975
RANCH-TEJON-2	June-July 1978

HORIZONTAL OBSERVATION ANALYSIS

This supplement differs from previous supplements in several ways. The primary difference is that by using an experimental system to mathematically model the horizontal crustal motion, several epochs of data can now be adjusted simultaneously. Thus, this supplement reports not on the findings of a single epoch of data as before, but instead, on the results of combining the 10 individual RANCH-TEJON network surveys into a single simultaneously adjusted survey.

In the mathematical model necessary for the simultaneous adjustment of the data, the region of study consists of one or more subregions where existing fault lines provide the usual boundaries between the subregions. The latitude ϕ_t and the longitude λ_t of a geodetic station in the i^{th} subregion at time t are given by the formulas:

$$\begin{aligned} \phi_t &= \phi_{t_o} + f_{i,1}(t-t_o) + f_{i,3}(t-t_o)^2 \\ \lambda_t &= \lambda_{t_o} + f_{i,2}(t-t_o) + f_{i,4}(t-t_o)^2 \quad . \end{aligned} \qquad (1)$$

Here t_o is a fixed time of reference, and $(\phi_{t_o}, \lambda_{t_o})$ are the geodetic coordinates of the station at time t_o. Each $f_{i,j}$ for $1 \leq j \leq 4$ is a function of the variables ϕ_t and λ_t and is of the form

$$f_{i,j}(\phi_{t_o},\lambda_{t_o}) = b_{i,j,1} + b_{i,j,2}\phi_{t_o} + b_{i,j,3}\lambda_{t_o} + b_{i,j,4}\phi^2_{t_o} + \dots \qquad (2)$$

Note that this equation models the motion as a continuous function of time and as a discontinuous function of position. Note, too, that the discontinuities occur along the boundaries between subregions. Using this model, existing horizontal survey data in the form of directions, distances, and azimuths from various epochs can now be adjusted to obtain the least-squares estimates for the unknown coordinates (ϕ_{t_o}, λ_{t_o}) and the unknown coefficients $b_{i,j,k}$. The advantages and disadvantages of using such a model are discussed in Snay and Gergen (1978).

Once this adjustment process has estimated the parameters of the above model, the results can be better understood when transformed and expressed in terms of strain parameters. Briefly explained, strain parameters are derived by modeling a small area of the Earth's surface as a two-dimensional plane. With the selection of a point of origin, the east and north directions define the positive axes of a Cartesian coordinate system for this plane. All points within the plane can then be assumed to have been displaced over time where a point's east and north movements are described by the variables U_E and U_N, respectively. The derivatives of these variables with respect to length in each direction (east and north) are denoted by adding the proper subscript to the variable; thus for the east direction, U_{EE} and U_{NE} are the respective derivatives of U_E and U_N, and for the north, U_{EN} and U_{NN}. The time derivative of any quantity is expressed by placing a dot above the variable (for example, $\dot{U}_E = d(U_E)/dt$) and two dots above a variable represent the second derivative with respect to time. Finally, the matrix

$$\begin{bmatrix} \dot{U}_{EE} & \dot{U}_{EN} \\ \dot{U}_{NE} & \dot{U}_{NN} \end{bmatrix}$$

is called the strain-rate matrix. A complete discussion of these and other strain parameters with respect to deformation of geodetic networks is given in Pope (1966).

In the adjustment process, observational errors are assumed to follow a normal distribution, and each horizontal observation is assigned a weight equal to the inverse square of its standard deviation. The standard deviations are determined from adopted operating procedures of the National Geodetic Survey (Schwarz 1978). Thus, if the model of the least-squares adjustment is correct, the weighted sum of the squares of the residuals, denoted VPV, has a chi-squared distribution with the appropriate degrees of freedom, df. Furthermore, the variance of unit weight, $\hat{\sigma}_o^2$ = VPV/df, has a chi-squared over degrees of freedom distribution, and its expected value is one. If this variance of unit weight is significantly different from one, then at least one of several errors may have been committed:

1. The observations may be weighted improperly.
2. The observational errors are not normally distributed with zero mean; for example, blunders may be present in the data.
3. The mathematical model is inappropriate.

To test for the possibility of errors in items one and two above, each epoch of data was adjusted individually to a model which contained no time parameters (only latitudes and longitudes are estimated). Table 3 lists the results of these adjustments. The $\hat{\sigma}_o^2$ value is below the 95-percent confidence interval for three epochs--1967, 1968, and 1969--and above for two epochs--1966 and 1978. Therefore, blunders, weighting problems, or both may exist. This possibility needs to be considered when interpreting the results of other adjustments that involve data from several epochs.

The bottom row of table 3 shows the results of adjusting all the data to a model with no time parameters. For the sake of comparison, these values also appear in table 4 under the adjustment 1 title. The $\hat{\sigma}_o^2$ value of this combined adjustment, being sufficiently high, indicates the model's need for time parameters even with the possibility of weighting or blunder problems. The next several adjustments attempt to discover the most appropriate model for the data.

Adjustment 2, as listed in table 4, again adjusted all 10 epochs of data to a one-region model, but with the exception that time parameters were included. This adjustment estimated 20 time parameters; that is, five $b_{i,j,k}$

Table 3.--Adjustments of individual epoch to a model with no time parameters

Epoch	Stations	VPV	DF	σ_0^2	95% confidence interval
1964	13	35.9	54	0.66	0.66 - 1.41
1965	13	30.8	37	0.83	0.60 - 1.50
1966	13	160.7	100	1.61	0.74 - 1.30
1967	6	20.0	44	0.46	0.63 - 1.46
1968	6	9.5	36	0.26	0.59 - 1.51
1969	6	10.3	39	0.27	0.61 - 1.49
1970	13	90.7	88	1.03	0.73 - 1.32
1972	18	241.3	208	1.16	0.82 - 1.20
1975	18	62.8	74	0.85	0.70 - 1.35
1978	18	581.3	278	2.09	0.84 - 1.17
All data	24	5588.0	1132	4.93	0.92 - 1.08

Table 4.--Adjustments of horizontal data to various models

Adjustment	Data	Stations	Subregions	Time parameters	Constraints	VPV	DF	σ_0^2
1	1964-78	24	NA	0	0	5588.0	1132	4.936
2	1964-78	24	1	20	0	3200.3	1112	2.878
3A	1964-78	24	3	44	0	2200.1	1088	2.023
3B	1964-78	24	3	44	12	2229.7	1100	2.027
3C	1964-78	24	3	44	13	2317.3	1101	2.105
4	1969-78	18	NA	0	0	1679.2	788	2.131
5A	1969-78	18	3	16	0	1432.8	772	1.856
5B	1969-78	18	3	16	1	1437.0	773	1.859
5C	1969-78	18	1	4	1	1574.6	785	2.006
5D	1969-78	18	3	16	0	1455.2	772	1.885
5E	1969-78	18	3	18	0	1401.1	770	1.820
5F	1969-78	18	3	18	1	1401.3	771	1.818

parameters contained in each of the four $f_{i,j}$ polynomials. (See eqs. 1 and 2.) Because the observed data contained no information about the velocity or acceleration of the coordinate system's point of origin, the constant term, $b_{i,j,1}$, for each polynomial was not estimated. This action left only the five parameters that are the coefficients of ϕ, λ, ϕ^2, $\phi\lambda$, and λ^2 in eq. 2 to be determined. Using the results of adjustments 1 and 2, a statistical F-test was made. The hypothesis tested was that all 20 coefficients are equal to zero.

$$F_{20,1113} = \frac{(5588.0-3200.3)/(1133-1113)}{3200.3/1113} = 41.5 \quad .$$

Because 41.5 is greater than the critical value $F_{20,1113} = 1.88$ for $\alpha = 0.01$, the hypothesis is rejected. In other words, one or more of the coefficients are significantly different from zero.

The model of adjustment 2 assumes that the motion changes continuously as a function of position, but the existence of geologic faults violates this assumption. Fault effects should therefore be included in the model. To establish the location of these faults, figure 1B was examined and the unadjusted observations were investigated for systematic changes over time. Figure 3 depicts by bold, wavy lines the fault model chosen.

These faults divide the RANCH-TEJON network into three subregions, each denoted with a Roman numeral. It should be noted that, for the model, the accuracy of the fault locations need only be sufficient to assign stations to their proper subregions. The six stations of TEJON-2 were also suspected of spanning a fault, although figure 1B gives no indication of this.

In adjustment 3A, as listed in table 4, all the data were adjusted to the three-subregion model previously described. For each subregion, coefficients of the four polynomials in eq. 1 were estimated; however, these $f_{i,j}$ coefficients involved different $b_{i,j,k}$ coefficients for each subregion as follows:

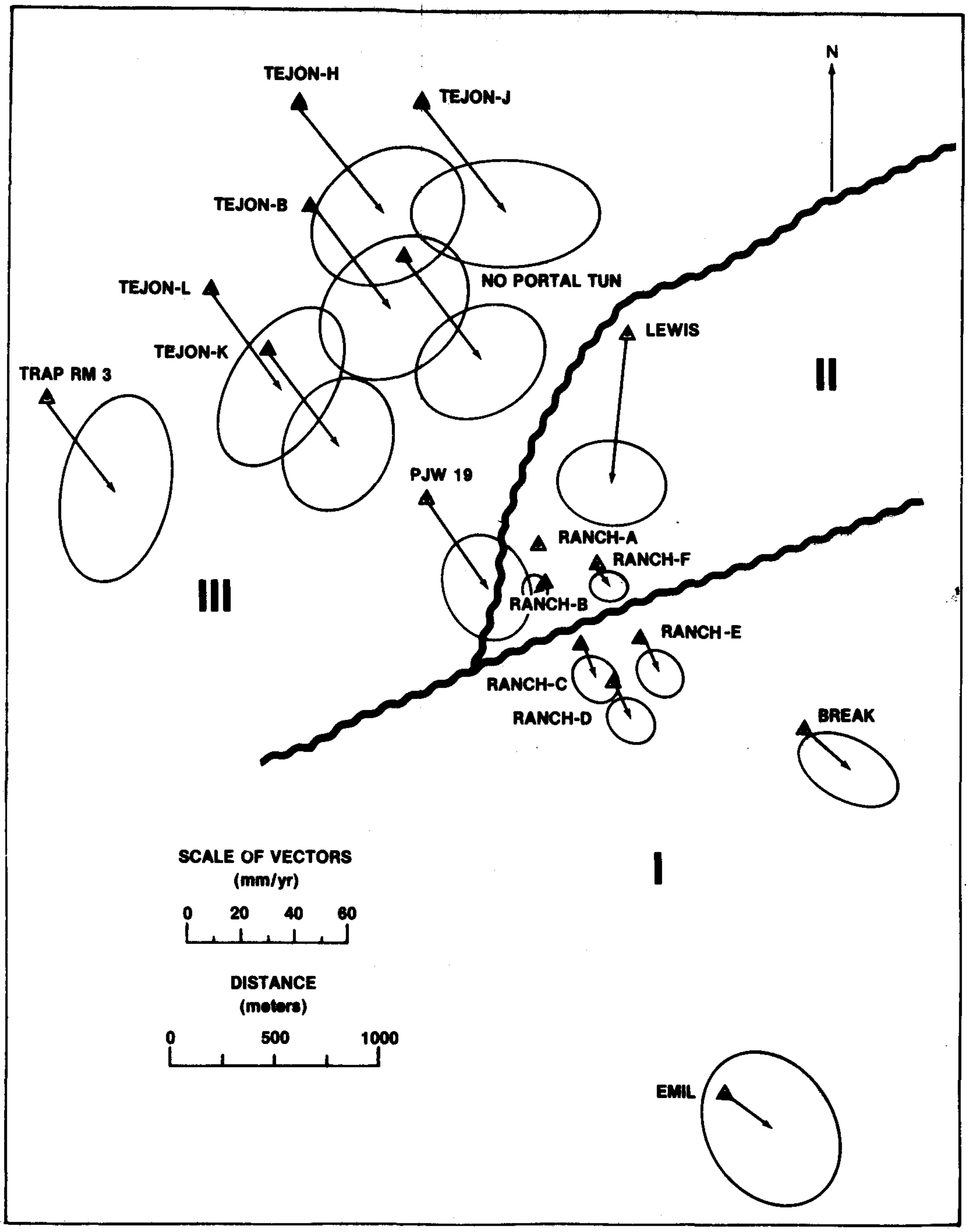

Figure 3.--Horizontal velocity vectors relative to RANCH-A and 95-percent confidence ellipses as obtained in adjustment 5F. The bold, wavy lines bound the three subregions of the model. The change in absolute orientation over time is constrained by requiring the strain-rate matrix of subregion I to be symmetric.

Subregion	Coefficients
I	ϕ, λ
II	constant, ϕ, λ
III	constant, ϕ, λ, ϕ^2, $\phi\lambda$, λ^2

The constant term for subregion I was neglected because this subregion contained the origin of the coordinate system. To test for a possible fault through the TEJON network, six terms were included in subregion III, allowing a greater variation of individual station movement.

Although the models of adjustments 2 and 3A are not directly comparable, the reduction in VPV from 3200.3 to 2201.3 by increasing the number of time parameters from 20 to 44 indicates that the three-subregion model of adjustment 3A is superior to adjustment 2's single-region model.

Adjustment 3B fits all 10 epochs of data to the same model as adjustment 3A, but with the exception that 12 constraints were imposed. These constraints held the coefficients of ϕ^2, $\phi\lambda$, and λ^2 in all four subregion III polynomials equal to zero. A statistical F-test can be used to test the hypothesis that these constraints are reasonable.

$$F_{12,1088} = \frac{(2229.7-2201.3)/(1100-1088)}{2201.3/1088} = 1.17 \quad .$$

Because 1.17 is less than the critical value $F_{12,1088} = 2.04$ for $\alpha = 0.01$, the hypothesis is accepted; thus if a fault exists through the TEJON network, the motion across it is below the level detectable with this test.

In adjustment 3C one additional constraint was imposed. This constraint held the acceleration in dilatation averaged over the three subregions equal to zero. Dilatation, Δ, is defined by the formula $\Delta = U_{EE} + U_{NN}$ and provides a first-order approximation to the changes in area of the Earth's surface resulting from deformation. This constraint can be represented by the formula $\ddot{\Delta}_1 + \ddot{\Delta}_2 + \ddot{\Delta}_3 = 0$, where the subscripts refer to the different subregions.

Adjustment 3C can be compared with adjustment 3B to test the hypothesis that this constraint is reasonable.

$$F_{1,1100} = \frac{(2317.3-2229.7)/(1101-1100)}{2229.7/1100} = 43.22 \quad .$$

Because 43.22 is greater than the critical value $F_{1,1100} = 6.63$ for $\alpha = 0.01$, the hypothesis is rejected; that is, the acceleration in dilatation averaged over the three subregions is significantly different from zero.

The preceding experiment indicates that terms which are nonlinear with respect to time cannot be neglected.

However, statistical correlations between the estimated coefficients of the $f_{i,j}$ polynomials indicate that the results obtained with the models of these adjustments are highly unreliable. In particular, for each i and k, the correlation between $b_{i,1,k}$ and $b_{i,3,k}$ is high, as is the correlation between $b_{i,2,k}$ and $b_{i,4,k}$. For all such pairings a value of -0.84 is obtained for the mean correlation. Thus, with both formulas of eq. 1, the linear terms are highly correlated with the nonlinear terms. Consequently, in the remaining adjustments, shorter time spans of data are used with models that are only linear with time.

The next set of adjustments seeks to model accurately the 1969-70 motion of the RANCH-TEJON-2 network.

Adjustment 4 fits these five epochs of data to a model without time parameters. This adjustment's variance of unit weight of 2.131 is relatively small compared with the value of 4.936 obtained from adjustment 1's 10-epoch model. This result, combined with the fact that the 1978 data adjustment alone yielded a $\hat{\sigma}_o^2$ value of 2.091 (table 3), suggests that the level of horizontal crustal motion in the 1969-78 period was relatively low.

Adjustment 5A fits the 1969-78 data to the three-subregion fault model previously described. For each subregion, coefficients of only the first two $f_{i,j}$ polynomials were estimated. The two polynomials which multiply the second power of time were omitted. The coefficients estimated for each subregion are:

Subregion	Coefficient
I	ϕ, λ
II	constant, ϕ, λ
III	constant, ϕ, λ

Adjustments 4 and 5A were compared to test the hypothesis that all 16 estimated time coefficients are zero.

$$F_{16,772} = \frac{(1679.2-1432.8)/(788-772)}{1432.8/772} = 8.30 \quad .$$

Because 8.30 is greater than the critical value $F_{16,772} = 2.0$ for $\alpha = 0.01$, the hypothesis is rejected; that is, at least one of the estimated coefficients is significantly different from zero.

Adjustment 5B is the same as adjustment 5A, but with the constraint added that the rate of rotation averaged over the three subregions is zero. For a subregion, the rotation, ω, is expressed by the formula $\omega = 1/2\ (U_{EN} - U_{NE})$, and the rotation represents the amount of absolute orientation change of the subregion resulting from deformation. This constraint is represented by the formula $\dot{\omega}_1 + \dot{\omega}_2 + \dot{\omega}_3 = 0$ where the subscripts refer to the different subregions. Adjustments 5A and 5B can be compared to test the hypothesis that this constraint is reasonable.

$$F_{1,772} = \frac{(1437.0-1432.8)/(773-772)}{1432.8/772} = 2.26$$

Because 2.26 is less than the critical value $F_{1,772} = 6.63$ for $\alpha = 0.01$, the hypothesis is accepted; that is, the network's rotation is too slight to be detected from the astronomic azimuth data available.

Adjustment 5C is the same as adjustment 5B, except that 12 additional constraints are included that (1) set the constant terms for subregions II and III equal to zero and (2) equate corresponding coefficients of different areas. This action is equivalent to fitting the 1969-78 data to a single symmetric strain-rate matrix that represents a one region model. Adjustments 5B and 5C can be compared to test the hypothesis that these 12 constraints are reasonable.

$$F_{12,773} = \frac{(1574.6-1437.0)/(785-773)}{1437.0/773} = 6.17 \quad .$$

Because 6.17 is greater than the critical value $F_{12,773} = 2.18$ for $\alpha = 0.01$, the hypothesis is rejected; that is, even with a shorter, linearly represented time span of data, the three-subregion model interprets the data better than the model of a single region.

In table 5 the strain-rate parameters estimated by both adjustment 5B's three-subregion model and those of adjustment 5C's single-region model are presented along with the strain-rate parameters from the 1973-78 data adjustment of the Tehachapi network (Savage et al. 1978). The Tehachapi network, which approximately covers the area shown in figure 1B, is one of several earthquake study trilateration networks observed by the U.S. Geological Survey. The Tehachapi observations are assumed to be adequately modeled by a single symmetric strain-rate matrix (Savage et al. 1978).

The disagreement in table 5 between the results of adjustment 5C and those obtained with the Tehachapi data do not necessarily contradict each other. Over such a local area as covered by the RANCH-TEJON network, the effects of motion along the faults dominate the more regional effects measured by the Tehachapi network. Indeed, when the fault effects are modeled out as in adjustment 5B, the strain-rate parameters belonging to the individual subregions should agree closer with those of the Tehachapi network. Within the accuracy limits of the estimates, this hypothesis proves to be true for subregions I and III; however, the strain-rate parameter for subregion II differs significantly from those of the Tehachapi network. Consequently, it is suspected that either a single strain-rate matrix inadequately models subregion II or that station LEWIS should possibly be reassigned to subregion III. (See fig. 1B.)

Table 5.--Various estimates of strain-rate parameters in units of 10^{-6} strain per year. Error estimates represent one standard deviation.

Parameter		Adjustment 5B		Adjustment 5C	Tehachapi network
	I	II	III		
$\dot{\epsilon}_{EE} = \dot{U}_{EE}$	0.48 ± 0.62	0.52 ± 0.85	0.00 ± 0.33	-0.62 ± 0.22	0.00 ± 0.03
$\dot{U}_{EN}$	-0.48 ± 0.31	-0.20 ± 0.43	0.31 ± 0.29		
$\dot{U}_{NE}$	0.67 ± 0.55	-1.06 ± 0.62	0.02 ± 0.28		
$\dot{\epsilon}_{NN} = \dot{U}_{NN}$	-0.25 ± 0.49	-3.35 ± 0.48	-0.42 ± 0.34	-1.31 ± 0.19	-0.21 ± 0.03
$\dot{\epsilon}_{EN} = \frac{1}{2}(\dot{U}_{EN}+\dot{U}_{NE})$	0.10 ± 0.37	-0.63 ± 0.45	0.16 ± 0.14	-0.24 ± 0.10	0.04 ± 0.02

Adjustment 5D is equivalent to adjustment 5A, except that station LEWIS was assigned to subregion III instead of subregion II. Comparing the VPV values for the two adjustments indicates that the data are better modeled with LEWIS in the original subregion II.

Adjustment	Location of LEWIS	VPV
5A	II	1432.8
5D	III	1455.2

Adjustment 5E uses the five-epoch 1969-78 data to test if subregion II is adequately modeled by a strain-rate matrix which is a constant function of position. Adjustment 5E differs from 5A in only two respects: first, the coordinate origin has been relocated from station EMIL in subregion I to station RANCH-A in subregion II; the second and more important change is that in subregion II an extra coefficient for each of the two $f_{i,j}$ polynomials is estimated. The new coefficients are $b_{i,j,4}$ for the ϕ^2 terms. (See eq. 2.) Thus for each of the two $f_{i,j}$ polynomials of a subregion, the following coefficients are determined.

Subregion	Coefficients
I	constant, ϕ, λ
II	ϕ, λ, ϕ^2
III	constant, ϕ, λ

The results of the two adjustments, 5A and 5E, are compared to test the hypothesis that each of the coefficients of ϕ^2 belonging to subregion II's $f_{i,j}$ polynomials is equal to zero. (The origin change does not affect the test conclusions.)

$$F_{2,770} = \frac{(1432.8-1401.0)/(772-770)}{1401.0/770} = 8.635 \quad .$$

Because 8.635 is greater than the critical value $F_{2,770} = 4.61$ for $\alpha = 0.01$, the hypothesis is rejected, i.e., subregion II is better modeled by a strain-rate matrix that is a variable function of position. This conclusion does not guarantee that the motion of subregion II is adequately modeled by including the ϕ^2 term in the polynomials. Indeed, with a total of only four stations in subregion II, it would be presumptuous to stipulate this particular form of the model. Physically, the results might either be due to stresses growing from the way subregion II is wedged between two branches of the Garlock fault, or they may stem from an unmodeled fault lying within subregion II. This latter speculation is strengthened by figure 1B's depiction of a short offshoot fault segment that splits LEWIS from the RANCH stations.

Adjustment 5F is the same as adjustment 5E except that subregion I's rate of rotation is constrained to zero. These two adjustments are compared to test the hypothesis that the constraint is reasonable.

$$F_{1,770} = \frac{(1401.3-1401.0)/(771-770)}{1401.0/770} = 0.14 \quad .$$

Because 0.14 is less than the critical value $F_{1,770} = 6.63$ for $\alpha = 0.01$, the hypothesis is accepted.

Figure 3 illustrates both the velocity vectors obtained in adjustment 5F and each vector's corresponding 95-percent error ellipse. Recall that these results are gathered from only the 1969-78 data, that the vectors and error ellipses are relative to the assumption that RANCH-A has not moved, and that the rate of rotation of subregion I is also assumed to be zero. The values of the velocity vectors are listed in table 6.

The following experiment was designed to gain a closer look at specific parameters and their variation over time.

The data were divided in two ways: first, the area was cut down to leave only the six station RANCH network and, second, the total time span was segmented into three intervals. Five epochs of data are included in the 1964-68 time segment, three epochs in 1968-72, and three again in the 1972-78 section.

The fault model, shown in figure 4, divides the RANCH network into two subregions. In the adjustment of each time data set, the coordinate origin is placed at RANCH-A, assuming this station to be motionless, and the rate of

Table 6.--Velocity vectors obtained in adjustment 5F for 1969-78 time period. Error estimates represent one standard deviation.

Subregion	Station	$\dot{U}_E$ (mm/yr)	$\dot{U}_N$ (mm/yr)
I	BREAK	1.7 ± 0.7	-1.4 ± 0.5
I	EMIL	1.7 ± 1.0	-1.2 ± 1.2
I	RANCH-C	0.5 ± 0.4	-1.2 ± 0.4
I	RANCH-D	0.7 ± 0.4	-1.2 ± 0.4
I	RANCH-E	0.8 ± 0.4	-1.3 ± 0.4
II	RANCH-A	0.0 ± 0.0	0.0 ± 0.0
II	RANCH-B	-0.3 ± 0.3	-0.2 ± 0.3
II	RANCH-F	0.4 ± 0.3	-0.7 ± 0.3
II	LEWIS	-0.5 ± 0.7	-5.5 ± 0.7
III	PJW 19 CADWR	2.2 ± 0.7	-3.3 ± 0.7
III	TRAP RM 3	2.5 ± 1.0	-3.3 ± 1.4
III	TRAP	2.5 ± 1.0	-3.3 ± 1.4
III	TEJON-B	2.9 ± 1.1	-3.9 ± 1.0
III	TEJON-H	3.1 ± 1.2	-4.1 ± 1.1
III	TEJON-J	3.1 ± 1.2	-4.2 ± 1.0
III	TEJON-K	2.6 ± 0.9	-3.6 ± 0.9
III	TEJON-L	2.7 ± 0.9	-3.7 ± 1.1
III	NORTH PORTAL TUN-3	2.8 ± 0.9	-3.9 ± 0.9

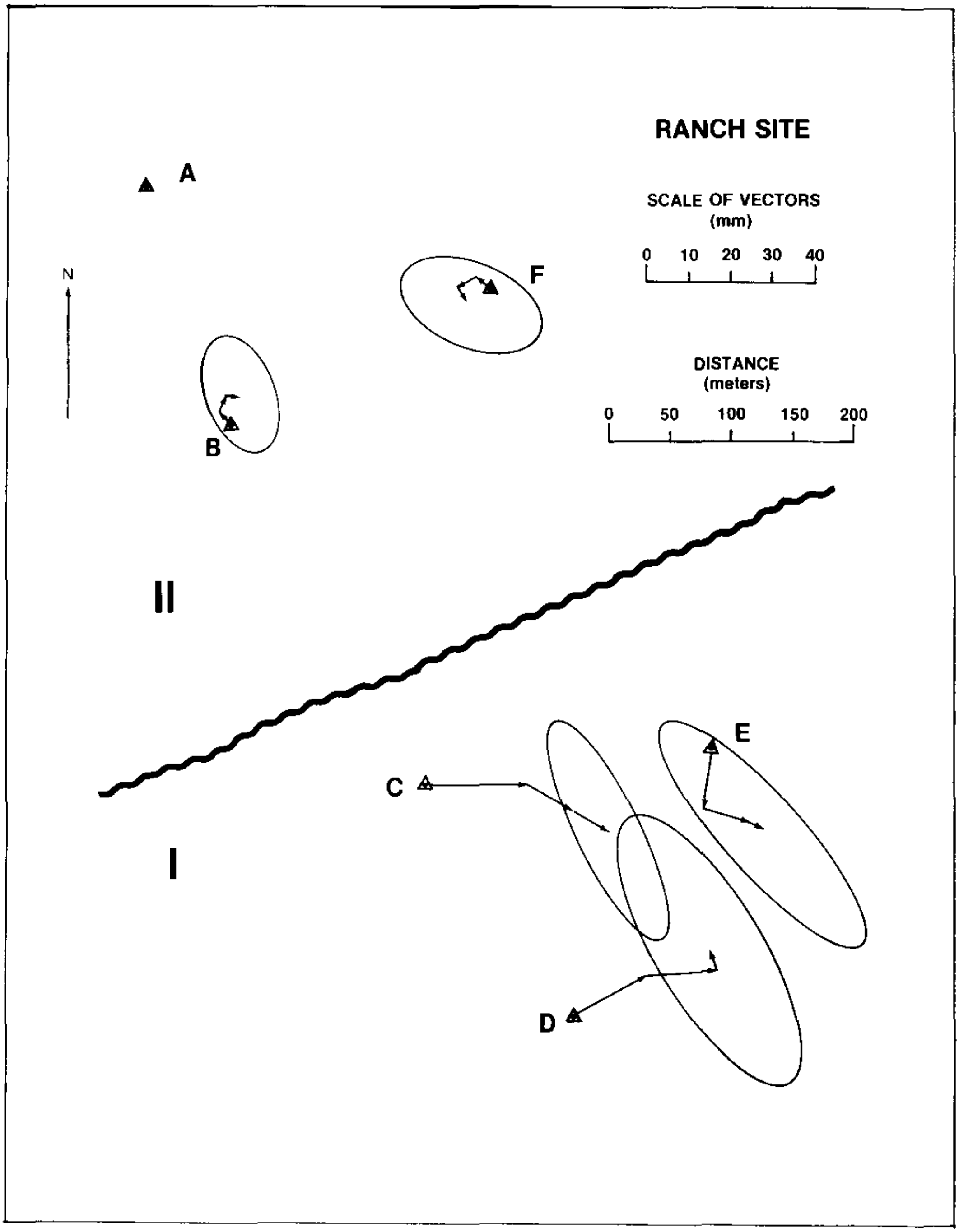

Figure 4.--Horizontal displacement vectors relative to RANCH-A for the three intervals 1964-68, 1968-72, and 1972-78. The 95-percent confidence ellipses correspond to the total displacement, 1964-78. The bold, wavy line separates the two subregions of the model. The change in absolute orientation over time is constrained by requiring the strain-rate matrix of subregion II to be symmetric for each time interval.

rotation of subregion II is assumed to be zero. The following coefficients of the two $f_{i,j}$ polynomials that multiply time to the first power were estimated:

Subregion	Coefficient
I	constant, ϕ, λ
II	ϕ, λ

Figure 4 illustrates the displacements of the RANCH stations for each of the three time intervals and also shows the 95-percent error ellipses associated with the total displacement, or equivalently, the resultant of the three vectors at each station. More detail of the relative motion of the RANCH stations is revealed in the vectors of figure 4 than in figure 3's velocity vectors. The vectors of figure 3 are smoothed to a greater degree because the subregions of adjustment 5F contain more stations extended over a greater area. Nevertheless, both figures expose two overall effects at the RANCH site: (1) a slight left-lateral shift at the fault, and (2) horizontal separation perpendicular to the fault between stations on opposite sides of the fault.

Table 7 lists various strain-rate parameters for each subregion and time interval. To compare these parameters with those of the Tehachapi network would yield questionable conclusions, because in the adjustment process the local effects on the strain parameters are smoothed or filtered out in covering the greater area of the Tehachapi network.

Although table 7 shows that the standard errors are generally the same magnitude as the estimated values, the results indicate that the strain rates fluctuate from period to period. This finding agrees with the earlier assertion in this report that the motion during the 1964-78 interval is inadequately modeled as a linear function of time.

From the results of this experiment, the surface slippage at the RANCH site can be estimated. The mean horizontal velocity of RANCH-B and RANCH-F, both stations north of the fault, was subtracted from the mean horizontal velocity

Table 7.--Strain-rate parameters of the RANCH network for three time intervals in units of 10^{-6} strain per year. Error estimates represent one standard deviation.

Parameter	Subregion I 1964-1968	Subregion I 1968-1972	Subregion I 1972-1978	Subregion II 1964-1968	Subregion II 1968-1972	Subregion II 1972-1978
$\dot{U}_{EE}$	-26.9 ± 3.4	-0.2 ± 3.4	-4.0 ± 1.1	-3.1 ± 4.4	-4.3 ± 3.9	1.7 ± 1.0
$\dot{U}_{EN}$	- 9.4 ± 1.5	-6.8 ± 1.9	6.5 ± 1.0	1.8 ± 1.1*	-4.3 ± 1.4*	-1.8 ± 0.6*
$\dot{U}_{NE}$	-11.5 ± 1.7	3.9 ± 2.0	2.6 ± 1.0	1.8 ± 1.1*	-4.3 ± 1.4*	-1.8 ± 0.6*
$\dot{U}_{NN}$	-19.2 ± 3.5	-7.3 ± 3.6	-8.2 ± 1.4	-2.5 ± 4.9	-9.4 ± 4.6	-0.3 ± 1.5
$\dot{\Delta} = \dot{U}_{EE} + \dot{U}_{NN}$	-46.1 ± 7.0	-7.5 ± 6.6	-12.1 ± 2.2	-5.6 ± 9.0	-13.7 ± 8.1	1.4 ± 2.1
$\dot{\omega} = \frac{1}{2}(\dot{U}_{EN} - \dot{U}_{NE})$	1.0 ± 1.2	-5.4 ± 1.4	1.9 ± 0.8	0*	0*	0*
$\dot{\gamma}_1 = \dot{U}_{EE} - \dot{U}_{NN}$	- 7.8 ± 1.9	7.1 ± 2.4	4.2 ± 1.2	-0.6 ± 2.5	5.1 ± 3.0	2.0 ± 1.4
$\dot{\gamma}_2 = \dot{U}_{EN} + \dot{U}_{NE}$	-20.9 ± 2.2	-2.9 ± 2.7	9.1 ± 1.3	3.6 ± 2.2	-8.6 ± 2.8	-3.6 ± 1.2

* By constraint.

of RANCH-C and RANCH-E, both to the south, for each of the three time intervals. For these calculations the strike of the fault is assumed to be N 60° E. Unless specified otherwise, all error estimates in the text represent one standard deviation.

Time interval	Rate of left-lateral strike-slip (mm/yr)	Rate of horizontal separation across the fault perpendicular to the strike (mm/yr)
1964-68	1.7 ± 0.5	3.8 ± 2.4
1968-72	1.7 ± 0.6	3.0 ± 2.0
1972-78	0.2 ± 0.3	0.6 ± 0.4

Because the stations located on opposite sides of the fault are moving apart, a normal-faulting mechanism is suggested.

VERTICAL OBSERVATION ANALYSIS

Leveling observations exist in four epochs covering the 1971-78 time period. Each epoch of data was adjusted separately holding the station TEJON-K fixed at the normal orthometric height of 1025.3290 meters. Table 8 lists each adjustment's results and also includes in the last column the rates of elevation change. These rate change values were obtained by fitting a straight line through each station's adjusted elevation values for the different epochs, and the corresponding standard errors for the rate estimates were derived from the residuals of the line fit. Figure 5 graphs these results. The vertical axis of each graph has been shifted so that the value 0.0 mm matches the station's adjusted elevation at the initial epoch.

Table 8 and figure 5 exhibit that height is adequately described as a linear function of time except at stations RANCH-C, RANCH-D, RANCH-E, and RANCH-F. This discrepancy from the linear model is possibly explained for the first three stations as being the result of their position across the southern branch of the Garlock fault relative to the rest of the network. Table 8 also points out that the RANCH stations, which lie to the south of the fault, are subsiding relative to those to the north. Subtracting the mean

Table 8.--Elevation changes at the RANCH-TEJON site

Station	Elevation 1971 (meters)	Elevation differences (mm) 7/1971 to 1/1972	1/1972 to 4/1975	4/1975 to 7/1978	Rate of elevation change (mm/yr) 1971 to 1978
TEJON K	1025.3290	0.0	0.0	0.0	0.0 ± 0.0
TEJON B	978.1815	1.9	1.8	9.8	1.8 ± 0.4
TEJON H	1070.6257*		3.7	9.2	2.0 ± 0.5
TEJON L	977.9023*		1.6	3.5	0.8 ± 0.2
NORTH PORTAL TUN 3	954.3553	1.2	4.3	5.3	1.5 ± 0.1
RANCH A	1047.0863	-0.9	5.0	5.7	1.5 ± 0.2
RANCH B	1007.2953	1.7	6.2	3.6	1.6 ± 0.3
RANCH F	1009.8473	3.7	13.6	2.2	2.8 ± 0.7
RANCH C	1037.8159	-3.6	9.8	-0.5	1.2 ± 0.6
RANCH D	1080.5688	-3.3	9.2	-3.5	0.7 ± 0.7
RANCH E	1064.3465	-1.5	10.5	-4.7	0.9 ± 0.8

*Measured in 1972.

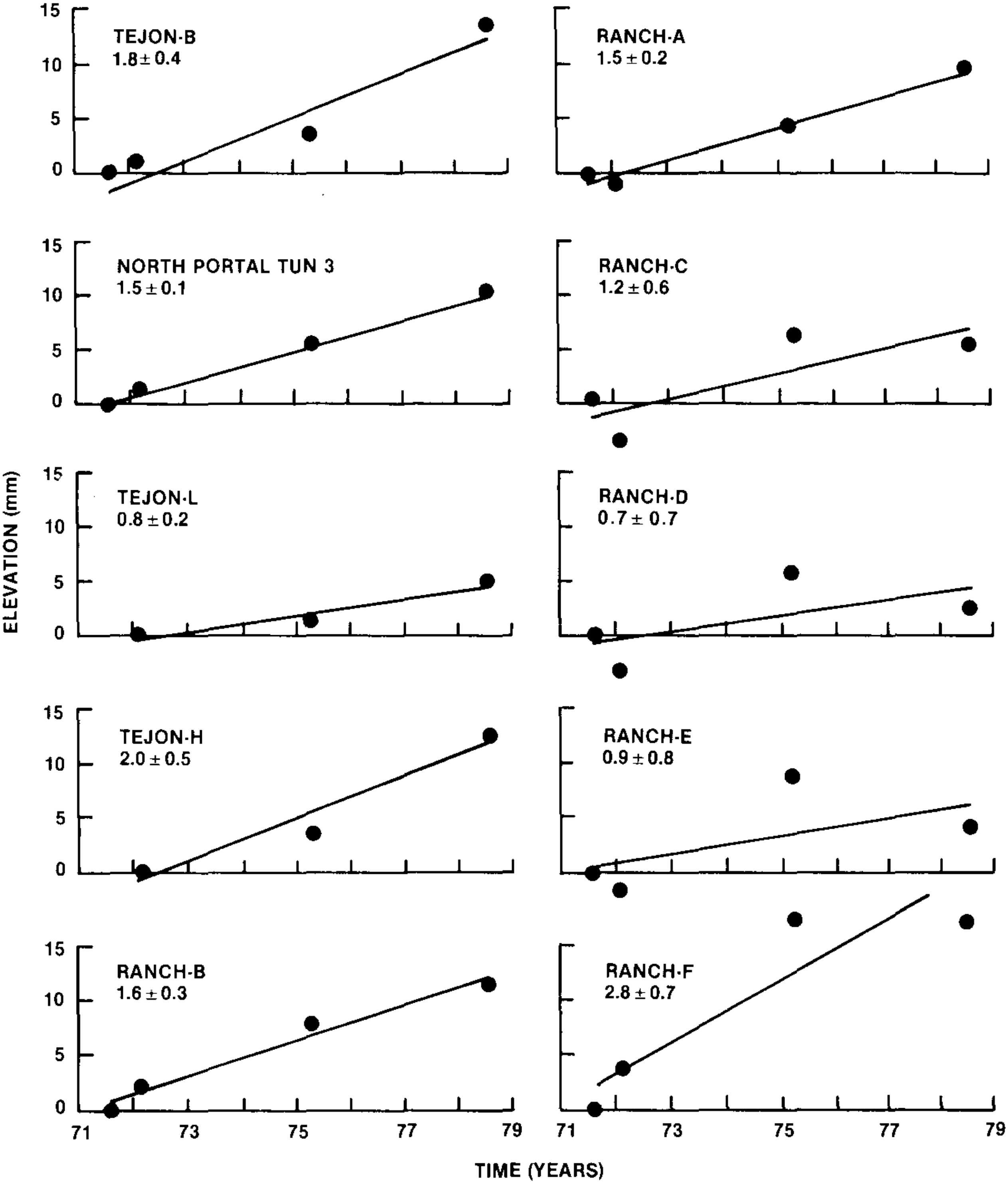

Figure 5.--Elevation changes relative to TEJON-K. The quoted rates and their standard deviations are in units of mm/yr.

vertical velocity of RANCH-B and RANCH-F from the mean vertical velocity of RANCH-C and RANCH-E yields 1.2 ± 0.6 mm/yr as the estimated subsidence rate during the 1971-78 time interval. The subsidence to the south, together with the normal-faulting mechanism, implies that the southern branch of the Garlock fault dips southward at the RANCH network.

SUMMARY

During the 1964-78 time span, the horizontal crustal motion in the RANCH-TEJON area has varied nonlinearly with respect to time. To gage this variation, data at the RANCH site were subdivided into three shorter time periods, each modeled linearly in time. During each interval, the branch of the Garlock fault spanned by the RANCH site exhibited left-lateral strike slip and dip slip corresponding to normal faulting. For both slip components, the rate of slippage decreases with time.

Horizontal data of the combined RANCH-TEJON-2 network for the 1969-78 time period were also modeled as a linear function of time. The data favor the inclusion of boundaries that divide the area into three subregions. This finding suggests that the existence and location of both branches of the Garlock fault significantly influence the nature of the movement. However, the data are sufficient only to assess the slippage along the southern branch. No fault activity within the area spanned by the six stations of TEJON-2 has been detected.

For the 1971-78 interval, vertical motion is adequately modeled as a linear function of time except, perhaps, at four stations; three of which lie south of the southern branch of the Garlock fault. Rates of subsidence indicate that the fault spanned by the RANCH site dips southerly.

ACKNOWLEDGMENT

The vertical data were adjusted by Samuel M. Reese, Jr., of the Vertical Network Branch, National Geodetic Survey.

REFERENCES

Federal Geodetic Control Committee, 1975: Specifications to Support Classification, Standards of Accuracy, and General Specifications of Geodetic Control Surveys. NOAA, NOS/NGS, Rockville, Md., 30 pp.

Federal Geodetic Control Committee, 1974: Classification, Standards of Accuracy, and General Specifications of Geodetic Control Surveys. NOAA, NOS/NGS, Rockville, Md., 12 pp.

Miller, Robert W., October 1976: Supplemental report no. 8--section IV: Sandburg to Wheeler Ridge, unpublished report, U.S. Department of Commerce (DOC), Coast and Geodetic Survey (C&GS), Rockville, Md.

________________, October 1972: Supplemental report no. 7--section IV: Sandburg to Wheeler Ridge, unpublished report, National Oceanic and Atmospheric Administration, DOC, C&GS, Rockville, Md.

________________, March 1970: Supplemental report no. 5--section IV: Sandburg to Wheeler Ridge, unpublished report, DOC, C&GS, Rockville, Md.

________________, September 1968: Supplemental report no. 4--section IV: Sandburg to Wheeler Ridge, unpublished report, DOC, C&GS, Rockville, Md.

________________, November 1967: Supplemental report no. 2--section IV: Sandburg to Wheeler Ridge, unpublished report, DOC, C&GS, Rockville, Md.

________________, October 1966: Supplemental report no. 1--section IV: Sandburg to Wheeler Ridge, unpublished report, DOC, C&GS, Rockville, Md.

Parkin, Ernest J., June 1966: Results of triangulation for Earth movement study at California aqueduct-fault crossing sites--section IV: Sandburg to Wheeler Ridge, unpublished report, DOC, C&GS, Rockville, Md.

Pope, A. J. (Dept. of Geodetic Science, The Ohio State University, Columbus), 1966: Strain analysis of repeated triangulation for the investigation of crustal movement. M.S. Thesis, 95 pp. Present address: NOAA, NOS/NGS, Rockville, Md.

Savage, J. C., Prescott, W. H., Lisowski, M., and King, N., 1978: Strain in southern California: measured uniaxial north-south regional contraction. Science, 202, 883-885.

Schwarz, C. R., 1978: The TRAV-10 horizontal network adjustment program. NOAA Technical Memorandum NOS NGS-12, DOC, NOAA, Rockville, Md., 52 pp. Available from National Technical Information Service, Springfield, Va. 22161 (item no. PB283087).

Snay, R. A., and Gergen, J. G., 1978: Monitoring regional crustal deformation with horizontal geodetic data. Proceedings of the Ninth GEOP Conference; Dept. of Geodetic Science Report No. 280, The Ohio State University, Columbus, Ohio, 87-92.

(Continued from inside front cover)

NOS NGS-3 Adjustment of geodetic field data using a sequential method. Marvin C. Whiting and Allen J. Pope, March 1976, 11 pp (PB253967). A sequential adjustment is adopted for use by NGS field parties.

NOS NGS-4 Reducing the profile of sparse symmetric matrices. Richard A. Snay, June 1976, 24 pp (PB-258476). An algorithm for improving the profile of a sparse symmetric matrix is introduced and tested against the widely used reverse Cuthill-McKee algorithm.

NOS NGS-5 National Geodetic Survey data: availability, explanation, and application. Joseph F. Dracup, Revised January 1979, 45 pp (PB80 118615). The summary gives data and services available from NGS, accuracy of surveys, and uses of specific data.

NOS NGS-6 Determination of North American Datum 1983 coordinates of map corners. T. Vincenty, October 1976, 8 pp (PB262442). Predictions of changes in coordinates of map corners are detailed.

NOS NGS-7 Recent elevation change in Southern California. S.R. Holdahl, February 1977, 19 pp (PB265-940). Velocities of elevation change were determined from Southern Calif. leveling data for 1906-62 and 1959-76 epochs.

NOS NGS-8 Establishment of calibration base lines. Joseph F. Dracup, Charles J. Fronczek, and Raymond W. Tomlinson, August 1977, 22 pp (PB277130). Specifications are given for establishing calibration base lines.

NOS NGS-9 National Geodetic Survey publications on surveying and geodesy 1976. September 1977, 17 pp (PB275181). Compilation lists publications authored by NGS staff in 1976, source availability for out-of-print Coast and Geodetic Survey publications, and subscription information on the Geodetic Control Data Automatic Mailing List.

NOS NGS-10 Use of calibration base lines. Charles J. Fronczek, December 1977, 38 pp (PB279574). Detailed explanation allows the user to evaluate electromagnetic distance measuring instruments.

NOS NGS-11 Applicability of array algebra. Richard A. Snay, February 1978, 22 pp (PB281196). Conditions required for the transformation from matrix equations into computationally more efficient array equations are considered.

NOS NGS-12 The TRAV-10 horizontal network adjustment program. Charles R. Schwarz, April 1978, 52 pp (PB283087). The design, objectives, and specifications of the horizontal control adjustment program are presented.

NOS NGS-13 Application of three-dimensional geodesy to adjustments of horizontal networks. T. Vincenty and B. R. Bowring, June 1978, 7 pp (PB286672). A method is given for adjusting measurements in three-dimensional space without reducing them to any computational surface.

NOS NGS-14 Solvability analysis of geodetic networks using logical geometry. Richard A. Snay, October 1978, 29 pp (PB291286). No algorithm based solely on logical geometry has been found that can unerringly distinguish between solvable and unsolvable horizontal networks. For leveling networks such an algorithm is well known.

NOS NGS-15 Goldstone validation survey - phase I. William E. Carter and James E. Pettey, November 1978, 44 pp (PB292310). Results are given for a space system validation study conducted at the Goldstone, Calif., Deep Space Communication Complex.

NOS NGS-16 Determination of North American Datum 1983 coordinates of map corners (second prediction). T. Vincenty, April 1979, 6 pp (PB297245). New predictions of changes in coordinates of of map corners are given.

NOS NGS-17 The HAVAGO three-dimensional adjustment program. T. Vincenty, May 1979, 18 pp (PB297069). The HAVAGO computer program adjusts numerous kinds of geodetic observations for high precision special surveys and ordinary surveys.

NOS NGS-18 Determination of astronomic positions for California-Nevada boundary monuments near Lake Tahoe. James E. Pettey, March, 1979, 22 pp (PB301264). Astronomic observations of the 120th meridian were made at the request of the Calif. State Lands Commission.

NOS NGS-19 HOACOS: A program for adjusting horizontal networks in three dimensions. T. Vincenty, July 1979, 18 pp (PB301351). Horizontal networks are adjusted simply and efficiently in the height-controlled spatial system without reducing observations to the ellipsoid.

NOS NGS-20 Geodetic leveling and the sea level slope along the California coast. Emery I. Balazs and Bruce C. Douglas, September 1979, 23 pp (PB80 120611). Heights of four local mean sea levels for the 1941-59 epoch in California are determined and compared from five geodetic level lines observed (leveled) between 1968-78.

NOS NGS-21 Haystack-Westford Survey. W. E. Carter, C. J. Fronczek, and J. E. Pettey, September 1979, 57 pp. A special purpose survey was conducted for VLBI test comparison.

NOS NGS-22 Gravimetric tidal loading computed from integrated Green's functions. C. C. Goad, October 1979, 15 pp. Tidal loading is computed using integrated Green's functions.

NOS NGS-23 Use of auxiliary ellipsoids in height-controlled spatial adjustments. B. R. Bowring and T. Vincenty, November 1979, 6 pp. Auxiliary ellipsoids are used in adjustments of networks in the height-controlled three-dimensional system for controlling heights and simplifying transformation of coordinates.

NOS NGS-24 Determination of the geopotential from satellite-to-satellite tracking data. B. C. Douglas, C. C. Goad, and F. F. Morrison, January 1980, 32 pp. The capability of determining the geopotential from satellite-to-satellite tracking is analyzed.

NOS NGS-25 Revisions of the HOACOS height-controlled network adjustment program. T. Vincenty, May 1980, 5 pp.

U.S. GOVERNMENT PRINTING OFFICE 1980 -311-046/229
(Continued on inside back cover)

(Continued)

NOAA Technical Reports, NOS/NGS subseries

NOS 65 NGS 1 The statistics of residuals and the detection of outliers. Allen J. Pope, May 1976, 133 pp (PB258428). A criterion for rejection of bad geodetic data is derived on the basis of residuals from a simultaneous least-squares adjustment. Subroutine TAURE is included.

NOS 66 NGS 2 Effect of Geoceiver observations upon the classical triangulation network. R. E. Moose and S. W. Henriksen, June 1976, 65 pp (PB260921). The use of Geoceiver observations is investigated as a means of improving triangulation network adjustment results.

NOS 67 NGS 3 Algorithms for computing the geopotential using a simple-layer density model. Foster Morrison, March 1977, 41 pp (PB266967). Several algorithms are developed for computing with high accuracy the gravitational attraction of a simple-density layer at arbitrary altitudes. Computer program is included.

NOS 68 NGS 4 Test results of first-order class III leveling. Charles T. Whalen and Emery Balazs, November 1976, 30 pp (GPO# 003-017-00393-1) (PB265421). Specifications for releveling the National vertical control net were tested and the results published.

NOS 70 NGS 5 Selenocentric geodetic reference system. Frederick J. Doyle, Atef A. Elassal, and James R. Lucas, February 1977, 53 pp (PB266046). Reference system was established by simultaneous adjustment of 1,233 metric-camera photographs of the lunar surface from which 2,662 terrain points were positioned.

NOS 71 NGS 6 Application of digital filtering to satellite geodesy. C. C. Goad, May 1977, 73 pp (PB-270192). Variations in the orbit of GEOS-3 were analyzed for M_2 tidal harmonic coefficient values that perturb the orbits of artificial satellites and the Moon.

NOS 72 NGS 7 Systems for the determination of polar motion. Soren W. Henriksen, May 1977, 55 pp (PB274698). Methods for determining polar motion are described and their advantages and disadvantages compared.

NOS 73 NGS 8 Control leveling. Charles T. Whalen, May 1978, 23 pp (GPO# 003-017-00422-8) (PB286838). The history of the National network of geodetic control, from its origin in 1878, is presented in addition to the latest observational and computational procedures.

NOS 74 NGS 9 Survey of the McDonald Observatory radial line scheme by relative lateration techniques. William E. Carter and T. Vincenty, June 1978, 33 pp (PB287427). Results of experimental application of the "ratio method" of electromagnetic distance measurements are given for high resolution crustal deformation studies in the vicinity of the McDonald Lunar Laser Ranging and Harvard Radio Astronomy Stations.

NOS 75 NGS 10 An algorithm to compute the eigenvectors of a symmetric matrix. E. Schmid, August 1978, 5 pp (PB287923). Method describes computations for eigenvalues and eigenvectors of a symmetric matrix.

NOS 76 NGS 11 The application of multiquadric equations and point mass anomaly models to crustal movement studies. Rolland L. Hardy, November 1978, 63 pp (PB293544). Multiquadric equations, both harmonic and nonharmonic, are suitable as geometric prediction functions for surface deformation and have potentiality for usage in analysis of subsurface mass redistribution associated with crustal movements.

NOS 79 NGS 12 Optimization of horizontal control networks by nonlinear programing. Dennis G. Milbert, August 1979, 44 pp (PB80 117948). Several horizontal geodetic control networks are optimized at minimum cost while maintaining desired accuracy standards.

NOS 82 NGS 13 Feasibility study of the conjugate gradient method for solving large sparse equation sets. Lothar Grundig, February 1980, 22 pp (PB80 180235). Method is suitable for constrained adjustments of triangulation networks but not for free adjustments.

NOS 83 NGS 14 Tidal corrections to geodetic quantities. P. Vanicek, February 1980, 30 pp (PB80 189376) Corrections for tidal force are formulated and tidal aspects relating to geodesy are discussed.

NOS 84 NGS 15 Application of special variance estimators to geodesy. John D. Bossler and Robert H. Hanson, February 1980. Special variance estimators, one involving the use of noninteger degrees of freedom, are analyzed and applied to least-square adjustments of geodetic control networks to determine their effectiveness.

NOS 85 NGS 16 The Bruns transformation and a dual setup of geodetic observational equations. Erik W. Grafarend, April 1980, 73 pp (PB80 202302). Geometric and physical observations are combined within a unified theoretical framework.

NOS 86 NGS 17 On the weight estimation in leveling. P. Vanicek and Erik W. Grafarend, May 1980, 36 pp.

NOAA Manuals, NOS/NGS subseries

NOS NGS 1 Geodetic bench marks. Lt. Richard P. Floyd, September 1978, 56 pp (GPO# 003-017-00442-2) (PB296427). Reference guide provides specifications for highly stable bench marks, including chapters on installation procedures, vertical instability, and site selection considerations.

U.S. DEPARTMENT OF COMMERCE
National Oceanic and Atmospheric Administration
National Ocean Survey
National Geodetic Survey, OA/C18x2
Rockville, Maryland 20852

OFFICIAL BUSINESS

POSTAGE AND FEES PAID
U.S. DEPARTMENT OF COMMERCE
COM-210

PRINTED MATTER

U.S.MAIL ®